Original Article

MOLECULAR METABOLISM

Beta cell specific cannabinoid 1 receptor deletion counteracts progression to hyperglycemia in non-obese diabetic mice

Kanikkai Raja Aseer [1], Caio Henrique Mazucanti [2], Jennifer F. O'Connell [2], Isabel González-Mariscal [3], Anjali Verma [1], Qin Yao [2], Christopher Dunn [4], Qing-Rong Liu [2], Josephine M. Egan [2], Máire E. Doyle [2,*]

ABSTRACT

Objective: Type 1 diabetes (T1D) occurs because of islet infiltration by autoreactive immune cells leading to destruction of beta cells and it is becoming evident that beta cell dysfunction partakes in this process. We previously reported that genetic deletion and pharmacological antagonism of the cannabinoid 1 receptor (CB1) in mice improves insulin synthesis and secretion, upregulates glucose sensing machinery, favors beta cell survival by reducing apoptosis, and enhances beta cell proliferation. Moreover, beta cell specific deletion of CB1 protected mice fed a high fat high sugar diet against islet inflammation and beta cell dysfunction. Therefore, we hypothesized that it would mitigate the dysfunction of beta cells in the precipitating events leading to T1D.

Methods: We genetically deleted CB1 specifically from beta cells in non-obese diabetic (NOD; NOD RIP Cre^{+} *Cnr1*$^{fl/fl}$) mice. We evaluated female NOD RIP Cre^{+} *Cnr1*$^{fl/fl}$ mice and their NOD RIP Cre^{-} *Cnr1*$^{fl/fl}$ and NOD RIP Cre^{+} *Cnr1*$^{Wt/Wt}$ littermates for onset of hyperglycemia over 26 weeks. We also examined islet morphology, islet infiltration by immune cells and beta cell function and proliferation.

Results: Beta cell specific deletion of CB1 in NOD mice significantly reduced the incidence of hyperglycemia by preserving beta cell function and mass. Deletion also prevented beta cell apoptosis and aggressive insulitis in NOD RIP Cre^{+} *Cnr1*$^{fl/fl}$ mice compared to wild-type littermates. NOD RIP Cre^{+} *Cnr1*$^{fl/fl}$ islets maintained normal morphology with no evidence of beta cell dedifferentiation or appearance of extra islet beta cells, indicating that protection from autoimmunity is inherent to genetic deletion of beta cell CB1. Pancreatic lymph node T_{reg} cells were significantly higher in NOD RIP Cre^{+} *Cnr1*$^{fl/fl}$ *vs* NOD RIP Cre^{-} *Cnr1*$^{fl/fl}$.

Conclusions: Collectively these data demonstrate how protection of beta cells from metabolic stress during the active phase of T1D can ameliorate destructive insulitis and provides evidence for CB1 as a potential pharmacologic target in T1D.

Keywords Beta cell apoptosis; Beta cell proliferation; Cannabinoid 1 receptor; Insulitis; Islet of Langerhans; Type 1 diabetes

1. INTRODUCTION

Deterioration of beta cell function prior to or concomitant with immune infiltration is increasingly recognized as a key step in the pathogenesis of autoimmune type 1 diabetes (T1D) [1–4]. In the prediabetic stage of the mouse model of T1D, the non-obese diabetic mouse (NOD/ShiLtJ), increased demand for insulin places a stress on the beta cells that is met by increased insulin translation [1,2]. This, in turn, leads to unresolved ER stress, accumulation of misfolded proteins, activation of the unfolded protein response (UPR) and increased lysosomal degradation of granular proteins [4,5]. Protein degradation under such conditions can cause neo-antigens to be produced. ER and oxidative stress also results in upregulation of major histocompatibility antigen class 1 (MHCI) allowing for presentation of the neo-antigens to T cells. This results in aggressive insulitis, worsening beta cell function, and ultimately apoptosis of beta cells and hyperglycemia [6,7]. Our previous work demonstrated that pharmacological antagonism of the cannabinoid 1 receptor (CB1) and beta cell specific deletion of CB1 has a unique and versatile profile because it improves insulin synthesis and secretion, upregulates glucose sensing machinery, favors beta cell

[1]Department of Surgery, University of Maryland School of Medicine, Baltimore, MD 21201, USA [2]Laboratory of Clinical Investigation, National Institute on Aging, National Institutes of Health, Baltimore, MD 21224, USA [3]Inserm UMR1190 - Translational Research of Diabetes, Pôle recherche 3ème Ouest, 1, place de Verdun 59045 Lille Cedex, France [4]Laboratory of Molecular Biology & Immunology, National Institute on Aging, National Institutes of Health, Baltimore, MD 21224, USA

*Corresponding author. E-mail: doyleme@nih.gov (M.E. Doyle).

Abbreviations: 2-AG, 2-Arachidonoylglycerol; 5-HT, 5-hydroxytryptamine; B2M, β2 microglobulin; Bcl-2, B-Cell CLL/Lymphoma 2; CB1, Cannabinoid 1 receptor; GCK, Glucokinase; GIP, Glucose-dependent insulinotropic peptide; GLP-1, Glucagon-like peptide-1; GLP-1R, Glucagon-like peptide 1 receptor; GLUT2, Glucose transporter 2; HTR2B, 5-Hydroxytryptamine (Serotonin) Receptor 2B; MHCI, Major histocompatibility antigen class 1; NOD, Non-obese diabetic mouse; NOD RIP Cre^{+}*Cnr1*$^{fl/fl}$, beta cell-specific CB1 knockout NOD mouse; NOD RIP Cre^{-} *Cnr1*$^{fl/fl}$, wild-type Cre negative littermate with an intact CB1; NOD RIP Cre^{+} *Cnr1*$^{Wt/Wt}$, wild-type Cre positive littermate with an intact CB1; PDX-1, Pancreatic and duodenal homeobox 1; PKA, protein kinase A; TPH1, Tryptophan Hydroxylase 1; Treg T, regulatory cells; UPR, unfolded protein response

Received November 3, 2023 • Revision received February 21, 2024 • Accepted February 22, 2024 • Available online 28 February 2024

https://doi.org/10.1016/j.molmet.2024.101906

survival by reducing apoptosis under stressful conditions while also enhancing beta cell proliferation, especially in the context of heightened requirements for insulin synthesis and secretion [8–11]. Additionally, our beta cell specific CB1 knockout mouse was inherently protected against islet inflammation and beta cell dysfunction even when continuously fed a high fat high sugar diet [12]. So, the culminative empirical evidence favors beta cell robustness in the setting of loss of CB1 signaling in beta cells. Therefore, we hypothesized that deletion of CB1, a $G_{\alpha i}$-protein coupled receptor encoded by the *Cnr1* gene, in beta cells of NOD mice would confer protection from hyperglycemia in the setting of autoimmune insulitis.

2. MATERIALS AND METHODS

2.1. Generation of beta cell specific CB1 knockout NOD mouse (NOD RIP Cre^{+} *Cnr1*$^{fl/fl}$)

The animal care and experimental procedures were approved by the National Institute on Aging (NIA) Animal Care and Use Committee (Protocol # 443-LCI-2022): NIA is AAALAC accredited and is a specific pathogen free facility with restricted access. Mice were housed 4 to a cage with environmental enrichment in individually ventilated cages under a 12-hr light/dark cycle at 22±1 °C. The facility bedding is corncob-based which is autoclaved prior to use. All mice are given *ad libitum* access to water that was processed through a reverse osmosis hyper-chlorination system. Mice were fed with autoclaved standard Envigo rodent diets, 2018SX or 2019S (breeder ration) with *ad libitum* access: All mice were under the supervision of animal facility caretakers and veterinarians. Animals were randomized according to genotype and collection of data was blinded. Non-obese diabetic mice NOD/ShiLt-Tg(Ins2-cre)5Lt/LtJ (JAX #003855) referred to as NOD RIP-Cre throughout this manuscript, were obtained from The Jackson Laboratory (Bar Harbor, ME) [13]. Since the genomic integration site of the transgene in NOD RIP-Cre mice was not known, we carried out Targeted Locus Amplification [14] sequencing using mouse bone marrow cells (Cergentis' TLA technology, Utrecht, The Netherlands) and found the complete RIP-Cre-H2-Ea-ps transgene sequence that is integrated in mouse chromosome 8 (chr8:123529070-123656521bp) in a repeat rich region (see GenBank accession # ON568502 for details). NOD RIP Cre mice were crossed to *Cnr1* floxed mice (*Cnr1*$^{flox/flox}$) [12] for more than 10 generations. A SNP map genome scan was performed (The Jackson Laboratory) to confirm that the mice used to continue breeding for the study were on a ≥99% NOD background. We refer to this beta cell specific *Cnr1* knockout NOD mouse (*Cnr1*$^{flox/flox}$ NOD RIP Cre^{+}) as NOD RIP Cre^{+} *Cnr1*$^{fl/fl}$ throughout. The RIP-Cre was always maintained as hemizygous or a cross between NOD RIP Cre^{+} and NOD RIP Cre^{-} mice [13]. The NOD RIP Cre^{-} *Cnr1*$^{fl/fl}$ mice were always age-matched littermates that were Cre-negative (*Cnr1*$^{flox/flox}$ NOD RIP Cre^{-}, referred to as NOD RIP Cre^{-} *Cnr1*$^{fl/fl}$ throughout). All mice used in this report were females because 80% of females are known to develop insulitis and hyperglycemia; however, we did find that NOD RIP Cre^{+} *Cnr1*$^{fl/fl}$ males (about 20% of which get insulitis) were also protected from hyperglycemia (n = 20 mice per group, 5 separate groups of mice, studies carried out over 2.5 years). Body weight and blood glucose were monitored on a weekly basis until the female mice were at least 26–30 weeks old. Animals were eventually euthanized, after which pancreata was isolated and processed for further analysis.

2.2. JD-5037 administration

Eight-week-old female NOD/ShiLtJ mice were given JD-5037 (2 mg/kg, MedChemExpress, Monmouth Junction, NJ), an inverse agonist to the CB1, by oral gavage for 4 weeks followed by an intraperitoneal glucose tolerance test.

2.3. Metabolic studies

Intraperitoneal glucose tolerance tests (IPGTT) were performed at both 9 and 14 weeks in WT and NOD RIP Cre^{+} *Cnr1*$^{fl/fl}$ mice and 12 weeks in NOD/ShiLtJ mice. Mice were fasted overnight in clean cages before IP injection of glucose (1.5 g/kg body weight), and blood glucose was measured using an ACCU-CHEK glucometer (Roche Diagnostics, Indianapolis, IN) from tail-pricks at the indicated time points. Fasting plasma insulin was determined by ELISA (Crystal Chem Inc., Elk Grove Village, IL).

2.4. Flow cytometry

For intracellular FoxP3 staining pancreatic lymph node and splenic cells were stained and acquired on Symphony-analyzer (Becton Dickinson, Franklin Lakes, NJ) and analyzed with FlowJo version 10.0 (FlowJo, Ashland, OR). Anti-PE-Cy7 CD4 (GK1.5), anti-PE CD8α (53–6.7), anti- PerCP-Cy5.5 CD25 (PC61), and anti- Alexa-fluor-647 FoxP3 (FJK-16s) (from BD Biosciences, eBioscience or BioLegend) were used for the staining of cells. In brief, cells were incubated with FC block and stained with antibodies for surface marker. Dead cells were excluded using the eBioscience™ Fixable Viability Dye eFluor-780 (ThermoFisher Scientific, Waltham, MA). For intracellular staining, cells were permeabilized using the eBioscience™ FoxP3/transcription factor staining buffer set (ThermoFisher Scientific) and stained with anti-FoxP3 antibody. To evaluate T-, B- and myeloid cell subtypes in the pancreatic lymph node cell population we used a panel of markers shown in Supplemental Table 1.

2.5. Pancreatic islet isolation

Islets of Langerhans were isolated by collagenase digestion of exocrine pancreata as described before [12]. Briefly, pancreata were perfused via the common bile duct with 3 mL of collagenase P solution at 0.6 mg/mL (Roche Diagnostics) in cold phenol red-free Hanks' balanced salt solution (HBSS) with DNase before excision from the abdomen. The islets were removed from acinar tissue by digestion with collagenase at 37 °C for 17 min. After washing with cold HBSS, single islets were handpicked under a stereomicroscope. Islets were then assayed for immunoblotting or real-time PCR.

2.6. Immunoblot analysis

Islets were isolated and hand-picked in the manner described above. They were washed in PBS before being lysed in ice-cold RIPA buffer with protease inhibitors, sonicated (Qsonica, Newtown, CT), centrifuged at 13,000 rpm for 10 min at 4 °C, and the supernatant was collected. Protein lysates were resolved by SDS-PAGE and then electroblotted onto polyvinylidene difluoride (PVDF) membranes. The membranes were probed overnight at 4 °C using the primary antibodies (Electronic Supplemental Table 2) indicated followed by secondary antibodies conjugated to horseradish peroxidase (HRP) for 1 h at room temperature. Immunoblots were developed with Super Signal West Femto HRP substrate (ThermoFisher Scientific), exposed to HyBlot CL autoradiography film (Thomas Scientific, Swedesboro, NJ) and were imaged using an SRX-101 film processor (Konica Minolta Medical Imaging., Wayne, NJ). Protein bands were quantified using ImageJ software and normalized against that of GAPDH.

2.7. Real-time qPCR

Following isolation and handpicking of islets, the islets were washed and resuspended in RNAeasy Plus lysis buffer for total RNA extraction using a RNeasy Mini kit (Qiagen, Valencia, CA), as directed by the manufacturer.

The quality and purity of RNA were evaluated using a NanoDrop spectrophotometer (Thermo Fisher Scientific). Up to 1 μg of total RNA was reverse transcribed into cDNA using iScript cDNA synthesis kit (Bio-Rad, Hercules, CA). The resultant cDNA was diluted (2.5—10 times) according to target abundance. TaqMan Gene Expression Assays (Applied Biosystems, Foster City, CA) were utilized to perform quantitative RT-PCR to quantify mRNA levels for CB1 receptor (*Cnr1*, Assay ID Mm01212171_s1), Tryptophan hydroxylase 1 (*Tph1*, Assay ID Mm01202614_m1), and Serotonin receptor 2a (*Htr2a*, Assay ID Mm00555764_m1), using β-actin expression (*Actb*, Assay ID Mm00607939_s1) as an endogenous control gene for normalization. qPCR reactions were run using the StepOnePlus Real Time System's default program. The ΔΔCt method was used to determine the relative fold change.

2.8. Histology, immunohistochemistry, and immunofluorescence

Pancreata were fixed overnight in 4% PFA, paraffin-embedded, and 5 μm sections were examined in further detail. Sections (55—75 islets per group) stained with H&E were blindly scored for insulitis using the following grades: 0, normal islet morphology with no periinsulitis or insulitis; 1, periinsulitis (focal aggregation at one pole of the islet and in contact with the islet periphery); 2, non-aggressive insulitis (islet infiltration covering less than 50% of the islet area); and 3, aggressive insulitis (infiltration covering <50% of the islet) [15]. The morphometric analysis of the islet was carried out on a minimum of six sections that were 150—200 μm apart. Antigen retrieval was achieved by heating the dewaxed paraffin tissue sections (95 °C, 30 min) in boiling citrate buffer (10 mM, pH 6.0) before being blocked with TBS/5% normal goat serum. Sections were immunostained overnight at 4 °C using appropriate primary antibodies (Supplemental Table 1), and subsequently probed with secondary antibodies tagged with Alexafluor at room temperature for 1 h. The slides were counterstained with 4′, 6-diamidino-2-phenylindole (DAPI) to visualize nuclei, and then mounted with antifade mounting medium. Confocal microscopy was performed on a Carl Zeiss LSM880 confocal microscope. Images were quantified (islet area, β cell area, α cell area, % Ki67$^+$ β cells, and % TUNEL$^+$ β cells) with HALO software (V3.3.2541.285) using the Indica Labs- Islet FL module v1.3 (Indica Labs, Albuquerque, NM). B2M and 5-HT (Electronic Supplemental Table 1) were detected by immunohistochemistry. Briefly, after antigen retrieval and overnight incubation with the appropriate antibodies, sections were incubated with SignalStain Boost IHC Detection Reagent, Rabbit-HRP (Cell Signaling Technology, Danvers, MA), following manufacturer's directions. Sections were then incubated with SignalStain DAB Substrate Kit (Cell Signaling Technology), until desired stain intensity was achieved. Pancreata from E11 timed mated females (The Jackson Laboratory) were used as a positive control for 5-HT staining. TUNEL staining was performed using an *in-situ* death detection kit, TMR red per the manufacturer's directions (Cat# 12156792910, Millipore Sigma, Burlington, MA).

2.9. Membrane-based cytokine/chemokine array

Two membrane-based immunoassays were used: Mouse Cytokine Array Kit, Panel A (R&D Systems) and a mouse Th1/Th2/Th17 Array C1 (RayBiotech). Pooled whole-islet extracts were collected from at least five 9-week-old NOD RIP Cre$^-$ *Cnr1*$^{fl/fl}$ and NOD RIP Cre$^+$ *Cnr1*$^{fl/fl}$ mice, incubated with the membranes overnight, and they were analyzed for the expression of various cytokines and chemokines according to the manufacturer's instructions. The signal intensities of the spots were quantified by ImageJ (NIH).

2.10. RNAscope fluorescence *in situ* hybridization

Within 1 min of their removal from the body, freshly dissected mouse pancreata were snap frozen in liquid nitrogen, and then embedded in O.C.T. compound (Fisher Healthcare, Houston, TX) in cryomolds on crushed dry ice, and stored at −80 °C. Sections (12 μm) were obtained on a Leica CM1950 cryostat (Wetzlar, Germany) and then fixed with 10% neutral buffered formalin (NBF) at 4 °C for 15 min before hybridization and staining. Pretreatment of pancreatic sections, probe hybridizations, and multiplex labeling were performed according to the ACDbio RNAscope Multiplex Fluorescent Detection Kit v2 protocol (Advanced Cell Diagnostics, Inc. Newark, CA), with a shortened protease pretreatment (10 min) due to the rich content of endogenous pancreatic proteases. Multiple channel RNAscope probes of *Cnr1* (Probe-Mm-*Cnr1*, Cat# 420721-C1), *Ins2* (Probe-Mm-*Ins2*-C2 Cat# 497811-C2), were also ordered from ACDbio. Images were acquired using a Carl Zeiss LSM980 confocal microscope (Oberkochen, Germany). The negative control used for the ISH was a universal control probe targeting the *dapB* (4-hydroxy-tetrahydrodipicolinate reductase) gene from the *Bacillus subtilis* strain, and the positive controls were probes targeting *Ubc* (ubiquitin C), and *Polr2A* (DNA-directed RNA polymerase II subunit RPB1).

2.11. Statistical analysis

All data are depicted as mean ± SEM unless otherwise specified. Statistical analysis was performed using GraphPad Prism v8.0 (GraphPad Software, San Diego, CA). Unpaired two-tailed Student's t test or one-way ANOVA followed by Tukey's post-hoc test was used to assess statistical significance as appropriate. *P* values of less than 0.05 ($*P < 0.05$; $**P < 0.01$; $***P < 0.001$, $****P < 0.001$) were considered statistically significant.

3. RESULTS

To examine whether NOD mice exhibit a metabolic response to CB1 blockade as observed previously in mouse models of type 2 diabetes [8,12], female NOD/ShiLtJ mice were treated with a CB1 inverse agonist, JD5037 (2 mg/kg, daily oral gavage) [16], or vehicle from 8 weeks of age. An IPGTT (1.5g glucose/kg) of these mice 4 weeks later demonstrated significantly lower blood glucose levels in the NOD/ShiLtJ-JD5037 mice (Figure 1A). This encouraging result gave the impetus to generate a conditional beta cell-specific CB1 knockout NOD mouse (NOD RIP Cre$^+$ *Cnr1*$^{fl/fl}$). *Cnr1*-floxed mice (*Cnr1*$^{flox/flox}$ [12]) were backcrossed with NOD RIP-Cre [13] for >10 generations to achieve >99% NOD genetic background (see Research Design and Methods for detailed information and genetic testing). We have shown previously that *Cnr1* in islets is limited to beta cells [16] hence the very low level of expression of *Cnr1* in the NOD RIP Cre$^+$ *Cnr1*$^{fl/fl}$ can be attributed to a few ductal cells isolated with the islets. Islets extracted from NOD RIP Cre$^+$ *Cnr1*$^{fl/fl}$ mice had much lower levels of *Cnr1* transcript compared to their NOD RIP Cre$^-$ *Cnr1*$^{fl/fl}$ littermates (Figure 1B). Exclusive absence of *Cnr1* expression in beta cells of NOD RIP Cre$^+$ *Cnr1*$^{fl/fl}$ was confirmed by fluorescent *in situ* hybridization (FISH) but *Cnr1* was clearly present in pancreatic ducts: *Cnr1* is not present in acinar tissue (Figure 1C,D, Supplemental Fig. 1A). Please see Supplemental Figs. 1B and C that show positive and negative controls for in *situ* hybridization). In agreement with observations on NOD/ShiLtJ mice [1] 14-week-old NOD RIP Cre$^-$ *Cnr1*$^{fl/fl}$ mice had higher blood glucose levels compared to 9-week-old animals: NOD RIP Cre$^+$ *Cnr1*$^{fl/fl}$ mice had no such deterioration in glucose tolerance (Figure 1E). Fasting (12+ hrs) insulin levels were higher, and more variable in NOD RIP Cre$^+$ *Cnr1*$^{fl/fl}$ mice (Figure 1F). Consistent with multiple reports female NOD RIP Cre$^+$ *Cnr1*$^{Wt/Wt}$ and NOD RIP Cre$^-$ *Cnr1*$^{fl/fl}$ mice developed severe hyperglycemia (blood glucose >600 mg/dL necessitating euthanasia) over the study period of 26 weeks while all the NOD RIP Cre$^+$ *Cnr1*$^{fl/fl}$ mice were protected (Figure 1G). Incidence and time of onset of hyperglycemia were

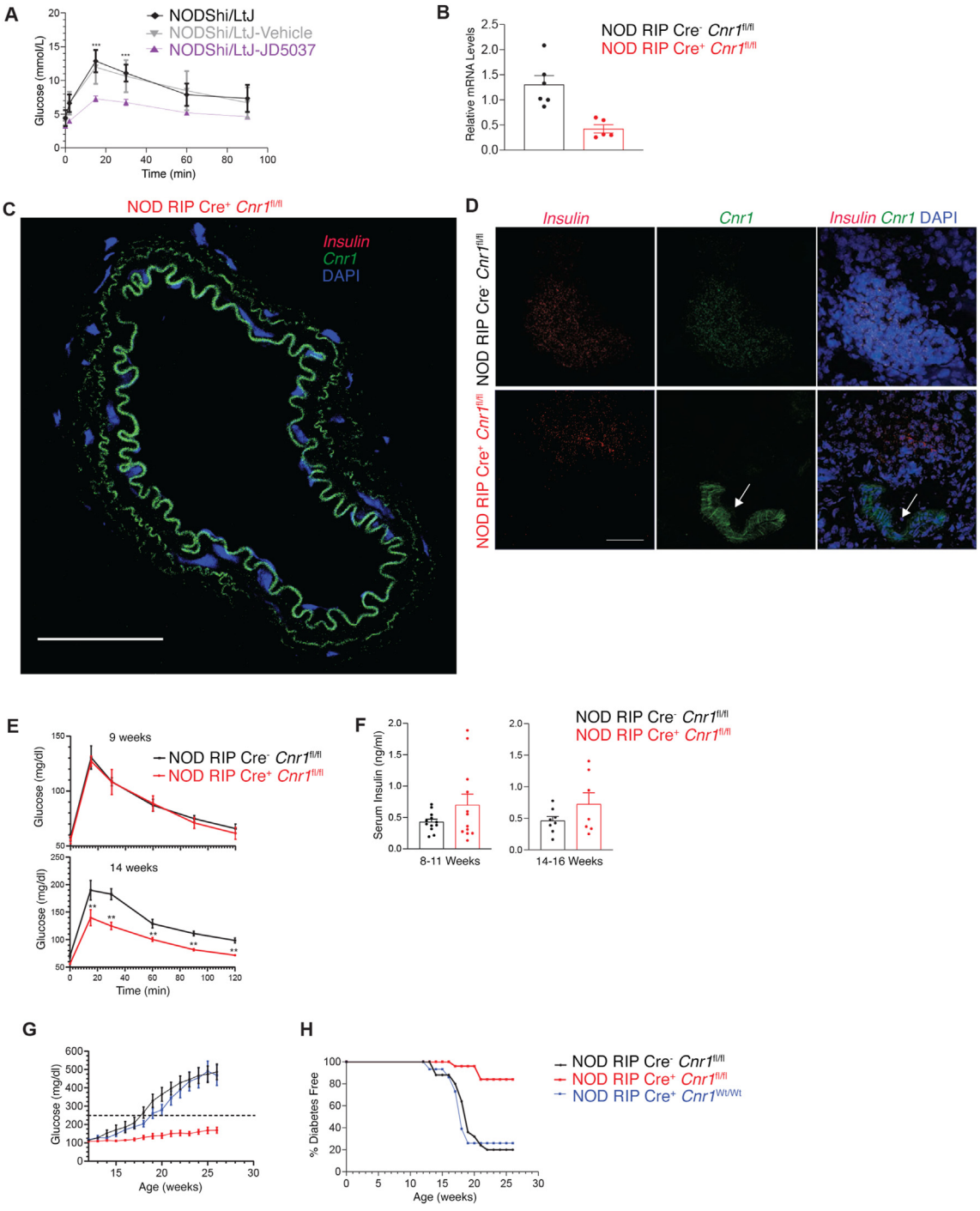

Figure 1: Beta cell specific deletion of CB1 in NOD mice (NOD RIP Cre^{+} *Cnr1*$^{fl/fl}$) lowers blood glucose levels and protects against progression to hyperglycemia in female NOD mice. (A) IPGTT (1.5 g/kg; age 12 weeks; n = 3 per condition) performed in NODShi/LtJ mice after treatment for 4 weeks with or without JD5037 (2 mg/kg) before the onset of diabetes. (**B**) *Cnr1* levels in isolated NOD RIP Cre^{-} *Cnr1*$^{fl/fl}$ (n = 6) and NOD RIP Cre^{+} *Cnr1*$^{fl/fl}$ (n = 5) islets were measured by RT-qPCR. **(C)** *In situ* hybridization image of a coronal section of the pancreatic duct of a NOD RIP Cre^{+} *Cnr1*$^{fl/fl}$ mouse pancreas *insulin* (red), *Cnr1* (green), and DAPI (blue). (**D**) Representative *in situ* hybridization images of *insulin* (red), *Cnr1* (green), and DAPI (blue) in pancreatic sections of NOD RIP Cre^{-} *Cnr1*$^{fl/fl}$ and NOD RIP Cre^{+} *Cnr1*$^{fl/fl}$ mice, showing co-expression of *insulin* and *Cnr1* in an islet from the NOD RIP Cre^{-} *Cnr1*$^{fl/fl}$ mice. White arrow indicates *Cnr1* is present in ductal cells of the NOD RIP Cre^{+} *Cnr1*$^{fl/fl}$ mice but is absent from an islet in the same section. **(E)** IPGTT (1.5 g/kg) of NOD RIP Cre^{-} *Cnr1*$^{fl/fl}$ and NOD RIP Cre^{+} *Cnr1*$^{fl/fl}$ mice at 9 (n = 7, n = 6 respectively) and 14 weeks of age (n = 6, both groups). **(F)** Fasting plasma insulin levels measured in both 8-11-week-old (n = 12) and 14–16-week-old NOD RIP Cre^{-} *Cnr1*$^{fl/fl}$ (n = 8) and NOD RIP Cre^{+} *Cnr1*$^{fl/fl}$ (n = 7) mice. **(G)** Weekly random blood glucose values NOD RIP Cre^{+} *Cnr1*$^{fl/fl}$ compared with their wild-type littermates NOD RIP Cre^{-} *Cnr1*$^{fl/fl}$ and NOD RIP Cre^{+} *Cnr1*$^{Wt/Wt}$. The dashed line shows the upper limit of normoglycemia. **(H)** Cumulative diabetes free percentages for NOD RIP Cre^{+} *Cnr1*$^{fl/fl}$ (n = 25) compared with their wild-type littermates NOD RIP Cre^{-} *Cnr1*$^{fl/fl}$ (n = 25) and NOD RIP Cre^{+} *Cnr1*$^{Wt/Wt}$ (n = 15). Data are presented as the mean ± SEM. $^{**}P < 0.01$. Scale bar = 50 μm. IPGTT = intraperitoneal glucose tolerance test.

similar in the NOD RIP Cre$^+$ *Cnr1*$^{Wt/Wt}$ and NOD RIP Cre$^-$ *Cnr1*$^{fl/fl}$ mice, with 80% having blood glucose approximating 600 mg/dL or were already euthanized by 26 weeks (Figure 1G). This indicates that the protective effects in NOD RIP Cre$^+$ *Cnr1*$^{fl/fl}$ mice were not due to RIP-Cre transgene. Thereafter NOD RIP Cre$^+$ *Cnr1*$^{fl/fl}$ and their NOD RIP Cre$^-$ *Cnr1*$^{fl/fl}$ littermates were used for all experiments. Four out of 25 NOD RIP Cre$^+$ *Cnr1*$^{fl/fl}$ mice had two non-consecutive blood glucose levels >250 mg/dl by 26 weeks of age representing a diabetes incidence of 16% (Figure 1H).

NOD RIP Cre$^+$ *Cnr1*$^{fl/fl}$ pancreatic morphology at 9 (Figure 2A–F) and 14 weeks (Supplemental Figs. 2A–F) were similar to published work on pharmacologic or global genetic inhibition of CB1 [8] and beta cell specific deletion of CB1 [16]. NOD RIP Cre$^+$ *Cnr1*$^{fl/fl}$ islets were larger (Figure 2A: 0.024 ± 0.002 *vs* 0.013 ± 0.001 mm^2, $P < 0.0001$) had increased beta cell area (Figure 2B 0.022 ± 0.001 *vs* 0.013 ± 0.001 mm^2, $P < 0.0001$) and proportionally increased alpha (α)-cell area (Figure 2C 0.004 ± 0.005 *vs* 0.006 ± 0.002 mm^2, $P < 0.0001$). NOD RIP Cre$^+$ *Cnr1*$^{fl/fl}$ islet morphology was preserved *i.e.* the islet core consisted of beta cells with no insulin/glucagon double-positive cells present (Figure 2D) and no obvious isolated insulin$^+$ cells in the exocrine pancreas or ducts of NOD RIP Cre$^+$ *Cnr1*$^{fl/fl}$ mice. The increased beta cell area was a consequence of significantly increased cell turnover as measured by the increased percentage of insulin$^+$/Ki67$^+$ cells per islet (Figure 2E,F: 3.12 ± 0.42 *vs* 1.09 ± 0.21%, $P < 0.0001$). By 14 weeks, there were no insulin$^+$/Ki67$^+$ cells in NOD RIP Cre$^-$ *Cnr1*$^{fl/fl}$ in islets infiltrated with immune cells (Supplemental Figs. 2E and F). The percentage insulin$^+$/Ki67$^+$ cells in large and normal NOD RIP Cre$^+$ *Cnr1*$^{fl/fl}$ islets at 60 weeks were similar to 9- and 14-week-old (Figure 2G, 3.2 ± 1.1%). There were very few terminal deoxynucleotidyl transferase dUTP nick end labelled (TUNEL)$^+$ beta cells (Figure 2H,I: 0.718 ± 0.218 *vs* 0.032 ± 0.032%, $P < 0.001$) in NOD RIP Cre$^+$ *Cnr1*$^{fl/fl}$ islets. Therefore, reduced apoptosis likely contributed to NOD RIP Cre$^+$ *Cnr1*$^{fl/fl}$ larger islet size. Previously we reported that CB1 activation inhibits beta cell proliferation in part through inhibition of the insulin/IRS1/2/pAkt pathway [8]. Levels of pIR$\beta_{1162/1163}$, pIRS1/2$_{612}$ and pAKT$_{473}$ in islets isolated from NOD RIP Cre$^+$ *Cnr1*$^{fl/fl}$ were significantly higher than in NOD RIP Cre$^-$ *Cnr1*$^{fl/fl}$ islets (Figure 2J). CB1 activation is reported to induce cleaved caspase-3 and negatively regulate the anti-apoptotic Bcl-2 molecules [10]. Protein levels of Bcl-2 were significantly higher in NOD RIP Cre$^+$ *Cnr1*$^{fl/fl}$ *vs* NOD RIP Cre$^-$ *Cnr1*$^{fl/fl}$ islets (Figure 2J). Reduced ER stress is a potential mechanism underlying protection against apoptosis in beta cells lacking CB1 [17]. Therefore, we measured protein levels of one of the most prominent unfolded protein response (UPR) signal transducers during ER stress. They are IRE1α [18] and activation (phosphorylation on Ser51) of the integrated stress response protein eIF2α as examined in 9-week-old NOD RIP Cre$^-$ *Cnr1*$^{fl/fl}$ and NOD RIP Cre$^+$ *Cnr1*$^{fl/fl}$ islets, and found that protein levels were significantly lower in the NOD RIP Cre$^+$ *Cnr1*$^{fl/fl}$ islets (Figure 2K).

Beta cell serotonin (5-HT) production is markedly elevated during pregnancy facilitating adaptation to insulin resistance and the increasing demand for insulin by inducing beta cell proliferation and improving glucose-induced insulin secretion [19]. Furthermore, there are reports of upregulated 5-HT production in beta cells of transgenic mice with insulin-promoter-linked-Cre transgenes that contain the growth hormone (hGH) cassette to enhance transgene expression. Our transgenic mice do not contain hGH (see Research Design and Methods) but there was still a theoretical possibility that transgenic mice lacking CB1 have increased beta cell turnover because its deficiency may activate lactogenic pathways. Transcript levels of the 5-HT synthesizing enzyme tryptophan hydroxylase 1 (*Tph1*) and the Gα_q-linked serotonin receptor *Htr2b* by which 5-HT mediates beta cell expansion and increased sensitivity to glucose [19] were similar in isolated islets from both genotypes (Supplemental Figs. 5A–D, n = 4 per genotype; Supplemental Fig. 5B shows confirmation of CB1 nullification). Embryonal day 11 pancreata were used as a positive control for 5-HT expression in beta cells [19]. Fourteen-week-old NOD RIP Cre$^-$ *Cnr1*$^{fl/fl}$ and NOD RIP Cre$^+$ *Cnr1*$^{fl/fl}$ islets had very little 5-HT compared to control (Supplemental Figs. 5E–G). Therefore, CB1 deficiency does not result in increased beta cell turnover through upregulation of *Tph1* nor does it improve beta cell glucose sensitivity by increased serotonergic response through *Htr2b*.

Evaluation of insulitis performed on whole pancreatic sections revealed characteristic immune infiltration [15] with lymphocytic invasion in islets of 26-week-old NOD RIP Cre$^-$ *Cnr1*$^{fl/fl}$ mice (Figure 3A–C). In contrast 80% of the islets evaluated in the age matched NOD RIP Cre$^+$ *Cnr1*$^{fl/fl}$ mice did not exhibit insulitis with only occasional peri-islet infiltration (13%). However, infiltration was not observed to invade or engulf NOD RIP Cre$^+$ *Cnr1*$^{fl/fl}$ islets (non-aggressive insulitis 6.5%) that were consistently large and well-preserved. Beta cell specific deletion of β2 microglobulin (B2M) demonstrates that while MHC class I presentation is not required for initiation of insulitis, there is some evidence that it is a component of progression to overt diabetes and hyperglycemia [20,21]. The transporters associated with antigen processing (TAPS 1,2) transport antigens to ER for loading onto MHCI [22,23]: TAPS protein amounts were significantly lower in protein extracts from NOD RIP Cre$^+$ *Cnr1*$^{fl/fl}$ islets (Figure 3D). GAD65 is a major beta cell target antigen for autoreactive CD8$^+$ T cells and a marker of beta cell death [24]. Protein extracts from 9-week-old NOD RIP Cre$^+$ *Cnr1*$^{fl/fl}$ islets had lower levels of CD8α and GAD65 (Figure 3D) than NOD RIP Cre$^-$ *Cnr1*$^{fl/fl}$ islets. Beta cells in NOD RIP Cre$^-$ *Cnr1*$^{fl/fl}$ islets had obvious B2M immunostaining in a heterogeneous manner whither or not insulitis was present and was independent of islet size (Supplemental Figs. 5H and I). In stark contrast, B2M staining was absent in NOD RIP Cre$^+$ *Cnr1*$^{fl/fl}$ islets, including those with peri-islet inflammation (Figure 3E, lower panel and Supplemental Figs. 5H and I).

Evaluation of key immune cells such as naive and effector CD4$^+$ T cells, CD8$^+$ T cells and T$_{reg}$ cells in the draining pancreatic lymph nodes (Figure 4A) revealed significantly higher numbers of T$_{reg}$ cells in 10-week-old NOD RIP Cre$^+$ *Cnr1*$^{fl/fl}$ mice (Figure 4A) and increased numbers of these cells in the spleens of these mice relative to their wild-type littermates. Numbers of pancreatic lymph node CD3$^+$CD8$^+$, CD3$^+$CD4$^+$, and CD3$^+$CD4$^-$CD8$^-$TCR$^+$ T cells, B cells and myeloid cells did not differ between NOD RIP Cre$^+$ *Cnr1*$^{fl/fl}$ mice and their wild-type littermates at 16 weeks of age (Supplemental Fig. 6). As cytokines released from beta cells can directly modulate the local immune environment we examined levels of cytokines, and chemokines using proteome profiler analysis in islets from 9-week-old mice of both genotypes (Figure 4B,C). We identified a significant shift in cytokine profiles in NOD RIP Cre$^+$ *Cnr1*$^{fl/fl}$ mice compared with NOD RIP Cre$^-$ *Cnr1*$^{fl/fl}$ wildtype littermates (Figure 4B,C). Importantly, the expression levels of 6 cytokines, including IFN-γ, IL-1β, IL-10, IL-12p70, IL-23p19, and TNF α were markedly reduced, whereas the levels of IL-7, IL-13, IL-17, M-CSF, IL-2, and TGF β1 were elevated substantially in the islets from NOD RIP Cre$^+$ *Cnr1*$^{fl/fl}$ mice (Figure 4B,C). The NOD RIP Cre$^+$ *Cnr1*$^{fl/fl}$ islets had downregulated levels of intracellular cell adhesion molecule (ICAM-1), CXCL10, CXCL9, CCL5, and MIP-3α, but protective CXCL12 was concurrently produced at higher levels (Figure 4B,C). Our current understanding of the mechanism underlying the protection from hyperglycemia and insulitis when CB1 is deleted specifically from only beta cells in NOD mice is outlined (Figure 5).

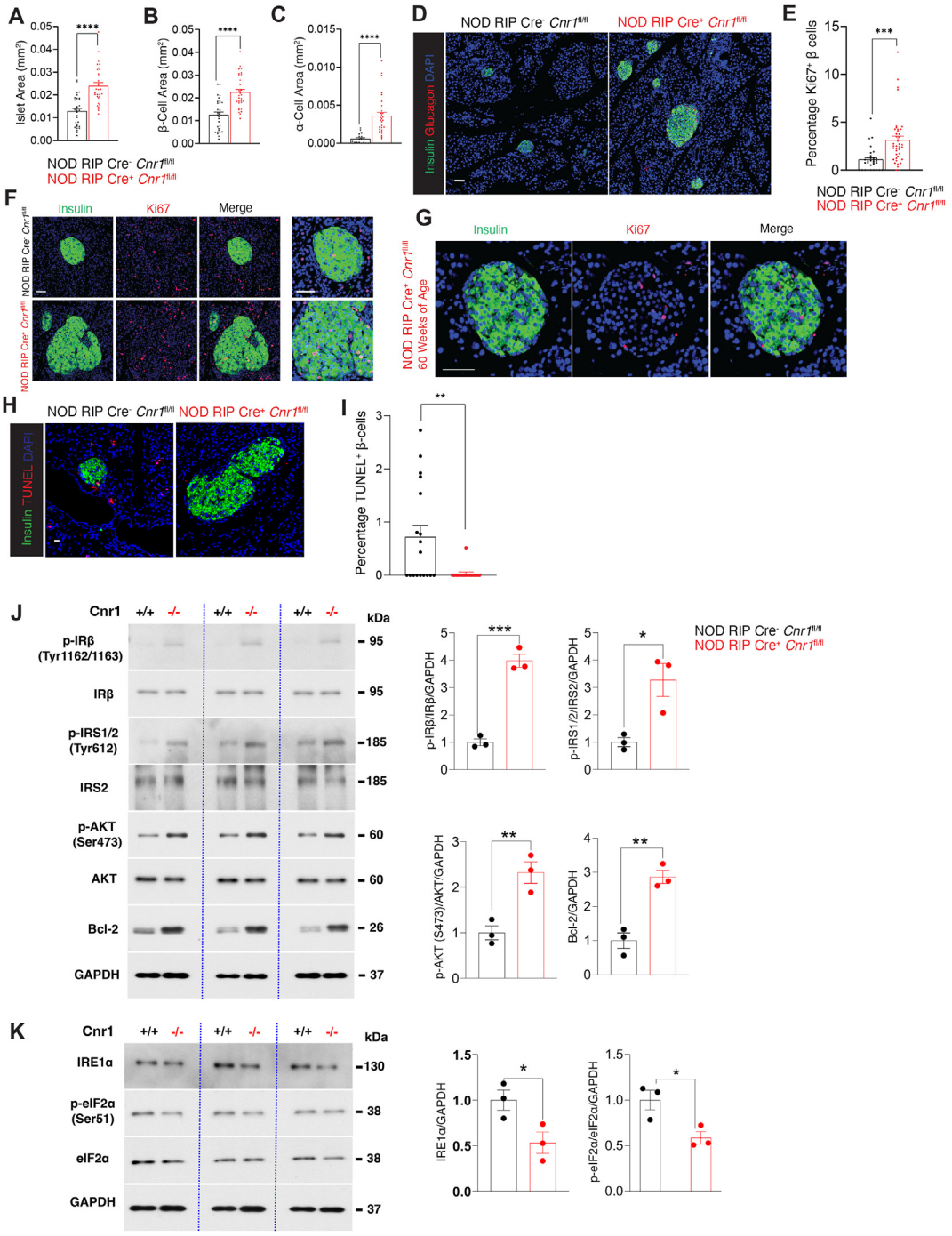

Figure 2: Beta cell specific ablation of CB1 in NOD mice increases islet area, enhances beta cell replication, and improves beta cell survival. Quantification of average islet area **(A)** beta cell mass (insulin) **(B)**: and α-cell mass (glucagon) **(C)** per islet for NOD RIP Cre^{-} *Cnr1*$^{fl/fl}$ (n = 18 islets) and NOD RIP Cre^{+} *Cnr1*$^{fl/fl}$ (n = 30 islets) at 9 weeks of age. **(D)** Representative pancreatic sections from NOD RIP Cre^{-} *Cnr1*$^{fl/fl}$ and NOD RIP Cre^{+} *Cnr1*$^{fl/fl}$ mice showing immunostaining of insulin (green), glucagon (red) and DAPI (blue). **(E)** Quantification of percentage of Ki67^{+} beta cells per islet for NOD RIP Cre^{-} *Cnr1*$^{fl/fl}$ and NOD RIP Cre^{+} *Cnr1*$^{fl/fl}$ mice at 9 weeks of age. **(F)** Representative image of staining Ki67 (red), insulin (green), and DAPI (blue) of an islet from a NOD RIP Cre^{-} *Cnr1*$^{fl/fl}$ and a NOD RIP Cre^{+} *Cnr1*$^{fl/fl}$ at 9 weeks of age showing increased numbers of Ki67 positive beta cells per islet in the NOD RIP Cre^{+} *Cnr1*$^{fl/fl}$ mice. **(G)** Representative image of an islet from a NOD RIP Cre^{+} *Cnr1*$^{fl/fl}$ at 60 weeks of age still showing Ki67^{+} beta cells. **(H)** Representative image of triple staining TUNEL (red), insulin (green), and DAPI (blue) showing an islet from a NOD RIP Cre^{-} *Cnr1*$^{fl/fl}$ and NOD RIP Cre^{+} *Cnr1*$^{fl/fl}$ mouse at 9 weeks of age. **(I)** Quantification of percentage beta cell apoptosis in NOD RIP Cre^{-} *Cnr1*$^{fl/fl}$ (n = 6) and NOD RIP Cre^{+} *Cnr1*$^{fl/fl}$ (n = 6) mice at 9 weeks of age. **(J)** Western blots and densitometry analysis of normalized p-IRβ, p-IRS1/2, p-AKT and Bcl-2 in islets isolated from NOD RIP Cre^{-} *Cnr1*$^{fl/fl}$ (n = 4) and NOD RIP Cre^{+} *Cnr1*$^{fl/fl}$ (n = 4) mice. **(K)** Western blots and densitometry analysis of normalized total IRE1α, eIF2α and p-eIF2α in extracts of islets isolated from NOD RIP Cre^{-} *Cnr1*$^{fl/fl}$ (n = 3) and NOD RIP Cre^{+} *Cnr1*$^{fl/fl}$ (n = 3) mice. Results are representative of at least three independent experiments. Graphical data show densitometry analyses normalized to GAPDH, total AKT, total IRS1/2, and/or total IRβ (loading controls). Data are presented as the mean ± SEM. $^{*}P < 0.05$, $^{**}P < 0.01$, $^{***}P < 0.001$, $^{****}P < 0.0001$. Scale bar = 50 μm. Complete original immunblots for J and K are provided in Supplemental Fig. 3.

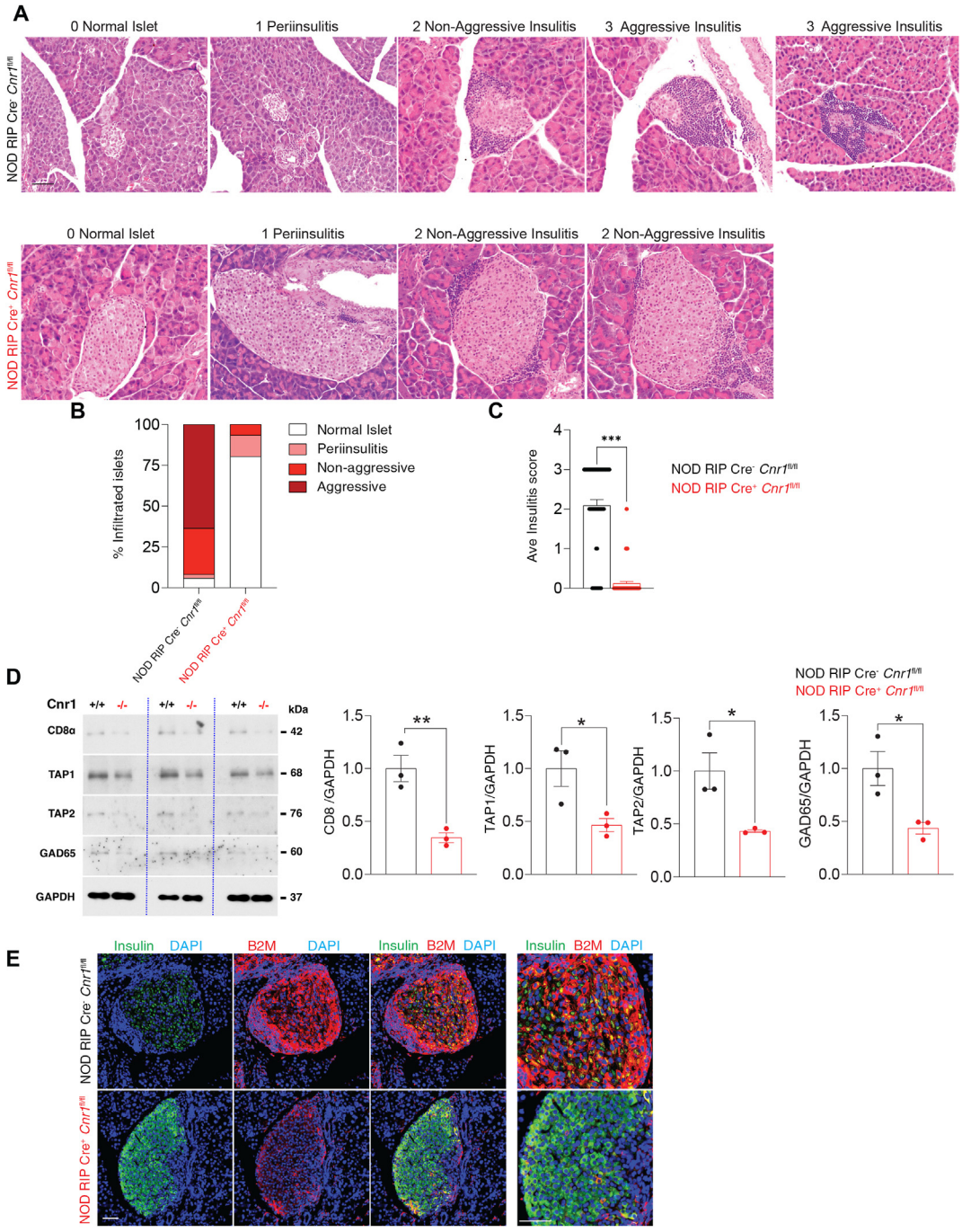

Figure 3: Beta cell specific CB1 deletion counteracts progression to hyperglycemia in NOD mice (A) Representative images of hematoxylin and eosin-stained islets from NOD RIP Cre^{-} *Cnr1*$^{fl/fl}$ and a NOD RIP Cre^{+} *Cnr1*$^{fl/fl}$ pancreata at 26 weeks of age in different stages of insulitis. **(B)** Quantitation of scoring of insulitis in NOD RIP Cre^{-} *Cnr1*$^{fl/fl}$ (n = 9 mice) and NOD RIP Cre^{+} *Cnr1*$^{fl/fl}$ (n = 7 mice) pancreata at 26 weeks of age. **(C)** The average insulitis score of NOD RIP Cre^{-} *Cnr1*$^{fl/fl}$ and NOD RIP Cre^{+} *Cnr1*$^{fl/fl}$ mice in **B**. **(D)** Western blots of CD8α, TAP1, TAP2, and GAD65 and densitometry analysis in pancreatic islets isolated from NOD RIP Cre^{-} *Cnr1*$^{fl/fl}$ (n = 4) and NOD RIP Cre^{+} *Cnr1*$^{fl/fl}$ (n = 4) mice. Results are representative of at least three independent experiments. Graphical data show densitometry analyses normalized to GAPDH (loading control). **(E)** Representative immunofluorescence staining for B2M (red) and insulin (green) in pancreatic sections of NOD RIP Cre^{-} *Cnr1*$^{fl/fl}$ and NOD RIP Cre^{+} *Cnr1*$^{fl/fl}$ at 14 weeks of age. Data are presented as the mean ± SEM. $^{*}P < 0.05$, $^{**}P < 0.01$, $^{***}P < 0.001$. Scale bar = 50 μm. Complete original immunoblots for D are provided in Supplemental Fig. 4.

4. DISCUSSION

Beta cells are not simply innocent bystanders targeted by a misguided autoimmune process but more likely they may even initiate or at least precipitate the cascade of events that lead to their demise [4,5,25]. The extremely high rate of insulin biosynthesis and protein processing in beta cells undergoing infiltration render them more susceptible to ER stress and the UPR [1–3]. Furthermore, beta cells are extremely susceptible to damage from reactive oxygen species (ROS) as they lack many critical antioxidant enzymes [5]. Altered proinsulin processing

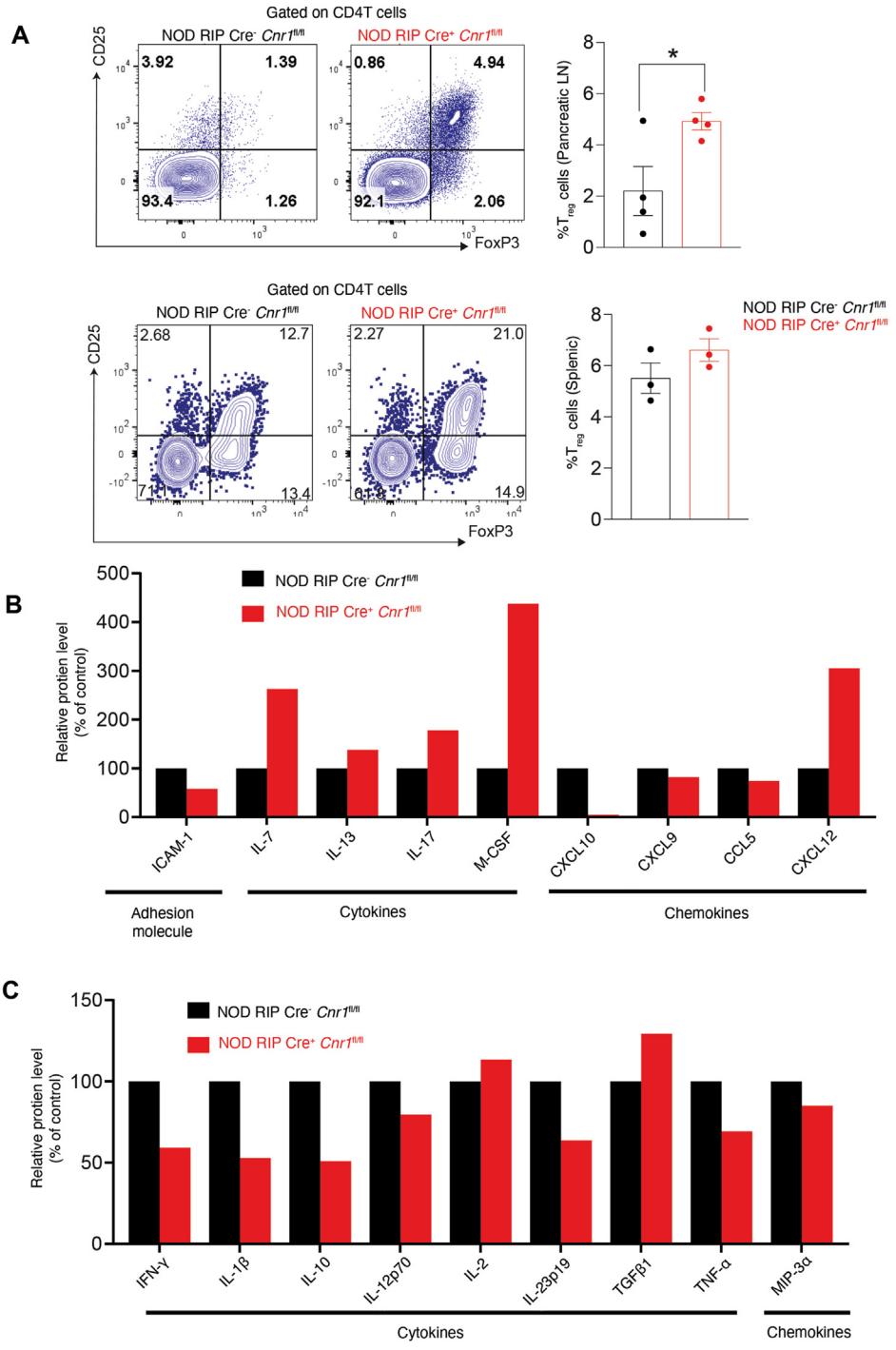

Figure 4: NOD RIP Cre^{+} *Cnr1*$^{fl/fl}$ mice have altered expression of signature markers associated with immune cell recruitment. (A) Flow cytometry analysis of regulatory T-cells (Tregs) for the surface expression of CD4, CD25 and intracellular expression of FoxP3 in pancreatic lymph nodes (top panel) of NOD RIP Cre^{-} *Cnr1*$^{fl/fl}$ (n = 4) and NOD RIP Cre^{+} *Cnr1*$^{fl/fl}$ (n = 4) mice and spleens (bottom panel) of NOD RIP Cre^{-} *Cnr1*$^{fl/fl}$ (n = 3) and NOD RIP Cre^{+} *Cnr1*$^{fl/fl}$ (n = 4) mice. Graphs shows the frequency of Tregs in pancreatic lymph nodes (top graph) and spleens (bottom graph) of NOD RIP Cre^{-} *Cnr1*$^{fl/fl}$ and NOD RIP Cre^{+} *Cnr1*$^{fl/fl}$ mice. The expression of cytokines and chemokines in extracts of islets from NOD RIP Cre^{-} *Cnr1*$^{fl/fl}$ mice and NOD RIP Cre^{+} *Cnr1*$^{fl/fl}$ mice (pooled from 5 mice for each genotype) was evaluated using the Mouse Cytokine Array Kit, Panel A (R&D) **(B)** and the mouse Th1/Th2/Th17 Array C1 (Raybiotech) (**C**). Differentially expressed cytokines (IFN-γ, IL-1β, IL-10, IL-12p70, IL-2, IL-23p19, TGFβ1, TNF-α, IL-7, IL-13, IL-17, M-CSF), chemokines (MIP-3α, CXCL10, CXCL9, CCL5, CXCL12) and adhesion molecule (ICAM-1) altered in NOD RIP Cre^{+} *Cnr1*$^{fl/fl}$ mice are highlighted. Cytokine and chemokine spots were measured and expressed as fold-changes as compared to NOD RIP Cre^{-} *Cnr1*$^{fl/fl}$ mice. Data are presented as the mean ± SEM. $^{*}P < 0.05$.

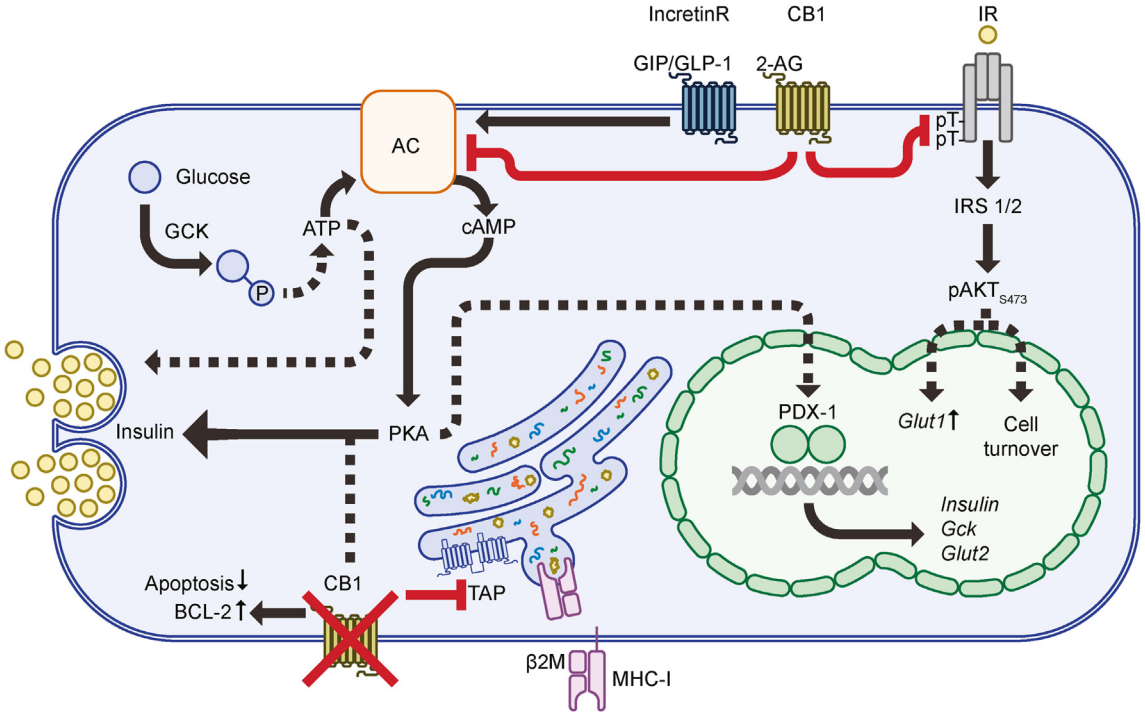

Figure 5: Schematic showing the pleotropic regulation of beta cell function, proliferation, and apoptosis by CB1 signaling. Activation of CB1 by ligands such as 2-AG suppresses insulin receptor (IR) signaling via IRS1,2/pAkt by diminishing IR kinase activity [8]. When CB1 is inhibited specifically in beta cells, phosphorylation of Akt at S473 is greatly increased, thereby allowing for increased GLUT1 transcription and translation and enhanced cell proliferation [12]. As CB1 is a $G\alpha_i$ coupled receptor its activation by the endogenous cannabinoids such as 2-AG inhibits adenylyl cyclase thereby blocking cAMP production [8]. Consequently, when CB1 signaling is inhibited intracellular cAMP levels increase [8,11]. This results in increased insulin secretion via enhanced PKA activity [16] that in turn increases protein levels of PDX-1, a transcription factor that has glucoregulatory, cytoprotective and proliferative actions in the beta cell. PDX-1 activation promotes *insulin*, *Gck* and *GLUT2* transcription. Moreover, CB1 activation is a negative modulator of incretin action. Incretin-mediated AC activation is also increased in response to CB1 inhibition thereby amplifying cAMP/PKA activity hence the proliferative and anti-apoptotic properties of incretins [11,41]. Finally, as we show in this report, beta cell specific genetic deletion of CB1 leads to significantly reduced beta cell apoptosis when it is under stress and prevents antigen presentation by MHCI on the cell surface. Glut2 = glucose transporter 2; PKA = protein kinase A; GLP-1 = glucagon-like peptide-1; GIP = glucose-dependent insulinotropic peptide; PDX-1 = pancreatic and duodenal homeobox 1; Gck = glucokinase; 2-AG = 2-arachidonoylglycerol; Bcl-2 = B-Cell CLL/Lymphoma 2.

both locally in the pancreas and in circulation in the pre-diabetic state of T1D correlate with immune markers and markers of beta cell stress, pointing to ongoing involvement of beta cell proteins in precipitating autoimmunity [25–27].

The majority of NOD RIP Cre^{+} *Cnr1*$^{fl/fl}$ mice were resistant to autoimmune attack as demonstrated by prevention of hyperglycemia in 84% of the animals at 26 weeks of age, and suppression of aggressive insulitis. This we attribute to the elevated numbers of pancreatic lymph node, FoxP3^{+}CD25^{+}Treg cells which can restore self-tolerance in T1D [28]. NOD RIP Cre^{+} *Cnr1*$^{fl/fl}$ islets exhibited lower levels of ER-stress with lower levels of IRE1α which has been previously shown to lower numbers of pancreatic CD8 cells because of reduced cross presentation [18]. However, the loss of IRE1α in the beta cell of NOD mice also led to a beta cell dedifferentiation phenotype, whereas the absence of CB1 signaling preserves and even enhances beta cell function as observed by increased intra-islet and serum insulin levels in the NOD RIP Cre^{+} *Cnr1*$^{fl/fl}$ mice. IRE is but one arm of the described three major branches of the UPR response to ER stress and previously published work indicates that the PERK/p-eIF2α arm is a more relevant way to assess ER status downstream of CB1 signaling. In rat mesangial cells high glucose induces apoptosis via ER stress which is mediated through CB1 activation of p-eIF2α as demonstrated using the CB1 antagonist AM251 which blocked activation of this pathway [29]. Likewise in human renal proximal tubular cells CB1 also mediates palmitic acid-induced apoptosis via p-eIF2α activation of ER stress [30]. Hence this led us to specifically examine levels of p-eIF2α (Ser51) in islets from the wild-type and NOD RIP Cre^{+} *Cnr1*$^{fl/fl}$ to begin to unravel the mechanism underlying CB1 induced ER-stress.

The improved beta cell health and absence of beta cell apoptosis observed in the NOD RIP Cre^{+} *Cnr1*$^{fl/fl}$ islets also leads to an more favorable islet cytokine profile with higher levels of TGFβ1, IL-2 and IL-7 all of which can induce peripheral Treg differentiation [28,31–33]. Evaluation of other key immune cell sub-types in wild type and knockout pancreatic lymph nodes showed no differences which is compatible with previous observations [34] and is indicative of more local islet effects on immune cell infiltrating populations [35]. All the mice used were hemizygous for Cre to avoid any reduction in insulitis observed by Leiter and co-workers with high levels of Cre expression [13]. While a limitation of our study is that we did not use the Cre^{+} wildtype control (NOD RIP Cre^{+} *Cnr1*$^{Wt/Wt}$) for all experiments we did monitor the blood glucose of these mice and found that 73% of them got hyperglycemia implying that the presence of Cre was not protective against insulitis.

In the context of other investigations of beta cell pathophysiology in T1D, boosting proliferation, preventing apoptosis, and targeting cell autonomous intracellular mechanisms that destroy or increase robustness of beta cells, in addition to immune modulators, are now emerging as potential strategies in a bid to prevent T1D. For example, using S961, an inhibitor of the insulin receptor that leads to insulin resistance in peripheral tissues and secondarily to beta cell

proliferation in NOD prevented progression to diabetes [34]. However, such a strategy to boost beta cells would be detrimental to every other cell type. Combining inhibition of DYRK1A, a protein kinase regulating cell proliferation, with TGFβ-SMAS signaling increased proliferation of human beta cells *in vitro* [36], but this would be a non-starter combination in humans because of off-target effects. It's also been proposed that dedifferentiated/degranulated beta cells, such as cells that express both glucagon and insulin as occurs with S961 treatment afford protection from generation of autoantigens and might have a role in later allowing for beta cell maturation [27]. Evidence for dedifferentiation of beta cells occurring in NOD RIP Cre^{+} $Cnr1^{fl/fl}$ mice was lacking because we did not find any islet cells expressing two hormones. Additionally, we do not see insulin-containing cells outside of islets as has also been seen with S961-driven increased beta cell turnover [34]; theoretically these non-islet cells might have different expression profiles and hence protection from T-cell activation.

One noteworthy finding, and not previously reported to our knowledge, is the clear presence of CB1 in ductal, but not acinar, cells. This is the first time this is being reported and therefore its function therein is unknown. One interesting avenue would be to investigate, for example, if CB1 downstream signaling is involved in the regulation of enzyme telomerase reverse transcriptase (Tert), a key enzyme in pancreatic cancer [37]. And CB1 may be involved in the secretory function of ducts such as control of carbonic anhydrase activity and/or cystic fibrosis transmembrane regulator, HCO^{-} secretion, as well as mucin secretion and production from goblet cells in ducts.

The beneficial effects from beta cell CB1 inhibition/nullification are numerous and include (Figure 5): Improved insulin synthesis and secretion and glucose sensing machinery [8,9]; decreased ROS formation [12]; improved IR/IRS1/2/AKT signaling; increased cell turnover and reduced apoptosis, especially under stress conditions from inflammation, high fat diets, and toxins [38–40]; reduced immune cell infiltration in islets - all in the setting of increased adenylyl cyclase activity due to lack of CB1 coupled $G_{i/o}$ [8,12] and improved incretin response [16]. A CB1 inhibitor to increase beta cell robustness and turnover, and a GLP-1 receptor agonist to improve autophagy and beta cell robustness even more, would seem strategies worth considering to prevent/delay insulin dependence in people who are on a path to have T1D in their future. Such a strategy would at least buy time for the need to use a second mechanistically distinct, immune target such as IL-2 therapy to expand T_{reg} cells.

DISCLOSURE

The authors have nothing to disclose.

CREDIT AUTHORSHIP CONTRIBUTION STATEMENT

Kanikkai Raja Aseer: Writing — original draft, Writing — review & editing, Visualization, Validation, Methodology, Investigation, Formal analysis, Data curation, Conceptualization. **Caio Henrique Mazucanti:** Visualization, Validation, Investigation, Formal analysis. **Jennifer F. O'Connell:** Visualization, Validation, Project administration, Investigation, Formal analysis, Data curation, Conceptualization. **Isabel González- Mariscal:** Investigation, Conceptualization. **Anjali Verma:** Visualization, Validation, Methodology, Investigation, Formal analysis. **Qin Yao:** Visualization, Validation, Methodology, Investigation. **Christopher Dunn:** Visualization, Validation, Methodology, Formal analysis. **Qing-Rong Liu:** Writing — original draft, Visualization, Validation, Supervision, Project administration, Methodology, Formal analysis. **Josephine M. Egan:** Writing — review & editing, Writing — original draft, Visualization, Validation, Supervision, Resources, Project administration, Methodology, Investigation, Funding acquisition, Formal analysis, Conceptualization. **Máire E. Doyle:** Writing — review & editing, Writing — original draft, Visualization, Validation, Supervision, Resources, Methodology, Investigation, Funding acquisition, Formal analysis, Data curation, Conceptualization.

ACKNOWLEDGMENTS

This work was funded by the Intramural Research Program of the National Institute on Aging, National Institutes of Health, USA. The authors especially Aaron Russell and Lauren Brick for help with Figure construction, especially the schema in Figure 5. We thank David Taylor for help in formatting and editing the figures and Shayna Yeager for help in editing the manuscript. We are beyond grateful to Brian Wilgenburg and the animal facility staff who maintained our mouse strains despite the hurdles placed during COVID.

DECLARATION OF COMPETING INTEREST

None.

DATA AVAILABILITY

Data will be made available on request.

APPENDIX A. SUPPLEMENTARY DATA

Supplementary data to this article can be found online at https://doi.org/10.1016/j.molmet.2024.101906.

REFERENCES

[1] Ize-Ludlow D, Lightfoot YL, Parker M, Xue S, Wasserfall C, Haller MJ, et al. Progressive erosion of β-cell function precedes the onset of hyperglycemia in the NOD mouse model of type 1 diabetes. Diabetes 2011;60(8):2086–91.

[2] Liang K, Du W, Zhu W, Liu S, Cui Y, Sun H, et al. Contribution of different mechanisms to pancreatic beta-cell hyper-secretion in non-obese diabetic (NOD) mice during pre-diabetes. J Biol Chem 2011;286(45):39537–45.

[3] Toren E, Burnette KS, Banerjee RR, Hunter CS, Tse HM. Partners in crime: beta-cells and autoimmune responses complicit in type 1 diabetes pathogenesis. Front Immunol 2021;12:756548.

[4] Carré A, Mallone R. Making insulin and staying out of autoimmune trouble: the beta-cell conundrum. Front Immunol 2021;12:639682.

[5] Leenders F, Groen N, de Graaf N, Engelse MA, Rabelink TJ, de Koning EJP, et al. Oxidative stress leads to β-cell dysfunction through loss of β-cell identity. Front Immunol 2021;12:690379.

[6] Serreze DV, Leiter EH, Christianson GJ, Greiner D, Roopenian DC. Major histocompatibility complex class I-deficient NOD-B2mnull mice are diabetes and insulitis resistant. Diabetes 1994;43(3):505–9.

[7] Wicker LS, Leiter EH, Todd JA, Renjilian RJ, Peterson E, Fischer PA, et al. Beta 2-microglobulin-deficient NOD mice do not develop insulitis or diabetes. Diabetes 1994;43(3):500–4.

[8] Kim W, Doyle ME, Liu Z, Lao Q, Shin YK, Carlson OD, et al. Cannabinoids inhibit insulin receptor signaling in pancreatic β-cells. Diabetes 2011;60(4):1198–209.

[9] Kim W, Lao Q, Shin YK, Carlson OD, Lee EK, Gorospe M, et al. Cannabinoids induce pancreatic β-cell death by directly inhibiting insulin receptor activation. Sci Signal 2012;5(216):ra23.

[10] Kim J, Lee KJ, Kim JS, Rho JG, Shin JJ, Song WK, et al. Cannabinoids regulate bcl-2 and cyclin D2 expression in pancreatic β cells. PLoS One 2016;11(3):e0150981.

[11] Shin H, Han JH, Yoon J, Sim HJ, Park TJ, Yang S, et al. Blockade of cannabinoid 1 receptor improves glucose responsiveness in pancreatic beta cells. J Cell Mol Med 2018;22(4):2337–45.
[12] González-Mariscal I, Montoro RA, Doyle ME, Liu QR, Rouse M, O'Connell JF, et al. Absence of cannabinoid 1 receptor in beta cells protects against high-fat/high-sugar diet-induced beta cell dysfunction and inflammation in murine islets. Diabetologia 2018;61(6):1470–83.
[13] Leiter EH, Reifsnyder P, Driver J, Kamdar S, Choisy-Rossi C, Serreze DV, et al. Unexpected functional consequences of xenogeneic transgene expression in beta-cells of NOD mice. Diabetes Obes Metabol 2007;9(Suppl 2):14–22.
[14] de Vree PJ, de Wit E, Yilmaz M, van de Heijning M, Klous P, Verstegen MJ, et al. Targeted sequencing by proximity ligation for comprehensive variant detection and local haplotyping. Nat Biotechnol 2014;32(10):1019–25.
[15] Flodström-Tullberg M, Yadav D, Hägerkvist R, Tsai D, Secrest P, Stotland A, et al. Target cell expression of suppressor of cytokine signaling-1 prevents diabetes in the NOD mouse. Diabetes 2003;52(11):2696–700.
[16] González-Mariscal I, Krzysik-Walker SM, Doyle ME, Liu QR, Cimbro R, Santa-Cruz Calvo S, et al. Human CB1 receptor isoforms, present in hepatocytes and β-cells, are involved in regulating metabolism. Sci Rep 2016;6:33302.
[17] Sahin GS, Lee H, Engin F. An accomplice more than a mere victim: the impact of β-cell ER stress on type 1 diabetes pathogenesis. Mol Metabol 2021;54:101365.
[18] Lee H, Lee YS, Harenda Q, Pietrzak S, Oktay HZ, Schreiber S, et al. Beta cell dedifferentiation induced by IRE1α deletion prevents type 1 diabetes. Cell Metabol 2020;31(4):822–836.e825.
[19] Kim H, Toyofuku Y, Lynn FC, Chak E, Uchida T, Mizukami H, et al. Serotonin regulates pancreatic beta cell mass during pregnancy. Nat Med 2010;16(7):804–8.
[20] Hamilton-Williams EE, Palmer SE, Charlton B, Slattery RM. Beta cell MHC class I is a late requirement for diabetes. Proc Natl Acad Sci U S A 2003;100(11):6688–93.
[21] de Jersey J, Snelgrove SL, Palmer SE, Teteris SA, Mullbacher A, Miller JF, et al. Beta cells cannot directly prime diabetogenic CD8 T cells in nonobese diabetic mice. Proc Natl Acad Sci U S A 2007;104(4):1295–300.
[22] Jackson DG, Capra JD. TAP1 alleles in insulin-dependent diabetes mellitus: a newly defined centromeric boundary of disease susceptibility. Proc Natl Acad Sci U S A 1993;90(23):11079–83.
[23] Qu HQ, Lu Y, Marchand L, Bacot F, Fréchette R, Tessier MC, et al. Genetic control of alternative splicing in the TAP2 gene: possible implication in the genetics of type 1 diabetes. Diabetes 2007;56(1):270–5.
[24] Hinke SA. Finding GAD: early detection of beta-cell injury. Endocrinology 2007;148(10):4568–71.
[25] Doliba NM, Rozo AV, Roman J, Qin W, Traum D, Gao L, et al. α Cell dysfunction in islets from nondiabetic, glutamic acid decarboxylase autoantibody-positive individuals. J Clin Invest 2022;132(11).
[26] Sims EK, Syed F, Nyalwidhe J, Bahnson HT, Haataja L, Speake C, et al. Abnormalities in proinsulin processing in islets from individuals with longstanding T1D. Transl Res 2019;213:90–9.
[27] Rui J, Deng S, Arazi A, Perdigoto AL, Liu Z, Herold KC. β cells that resist immunological attack develop during progression of autoimmune diabetes in NOD mice. Cell Metabol 2017;25(3):727–38.
[28] Li CR, Deiro MF, Godebu E, Bradley LM. IL-7 uniquely maintains FoxP3(+) adaptive Treg cells that reverse diabetes in NOD mice via integrin-β7-dependent localization. J Autoimmun 2011;37(3):217–27.
[29] Lim JC, Lim SK, Park MJ, Kim GY, Han HJ, Park SH. Cannabinoid receptor 1 mediates high glucose-induced apoptosis via endoplasmic reticulum stress in primary cultured rat mesangial cells. Am J Physiol Ren Physiol 2011;301(1):F179–88.
[30] Lim JC, Lim SK, Han HJ, Park SH. Cannabinoid receptor 1 mediates palmitic acid-induced apoptosis via endoplasmic reticulum stress in human renal proximal tubular cells. J Cell Physiol 2010;225(3):654–63.
[31] Chen W, Jin W, Hardegen N, Lei KJ, Li L, Marinos N, et al. Conversion of peripheral CD4+CD25- naive T cells to CD4+CD25+ regulatory T cells by TGF-beta induction of transcription factor Foxp3. J Exp Med 2003;198(12):1875–86.
[32] Grinberg-Bleyer Y, Baeyens A, You S, Elhage R, Fourcade G, Gregoire S, et al. IL-2 reverses established type 1 diabetes in NOD mice by a local effect on pancreatic regulatory T cells. J Exp Med 2010;207(9):1871–8.
[33] Bayer AL, Lee JY, de la Barrera A, Surh CD, Malek TR. A function for IL-7R for CD4+CD25+Foxp3+ T regulatory cells. J Immunol 2008;181(1):225–34.
[34] Dirice E, Kahraman S, De Jesus DF, El Ouaamari A, Basile G, Baker RL, et al. Increased β-cell proliferation before immune cell invasion prevents progression of type 1 diabetes. Nat Metab 2019;1(5):509–18.
[35] Boldison J, Hopkinson JR, Davies J, Pearson JA, Leete P, Richardson S, et al. Gene expression profiling in NOD mice reveals that B cells are highly educated by the pancreatic environment during autoimmune diabetes. Diabetologia 2023;66(3):551–66.
[36] Wang P, Karakose E, Liu H, Swartz E, Ackeifi C, Zlatanic V, et al. Combined inhibition of DYRK1A, SMAD, and trithorax pathways synergizes to induce robust replication in adult human beta cells. Cell Metabol 2019;29(3):638–652.e635.
[37] Neuhöfer P, Roake CM, Kim SJ, Lu RJ, West RB, Charville GW, et al. Acinar cell clonal expansion in pancreas homeostasis and carcinogenesis. Nature 2021;597(7878):715–9.
[38] Hennige AM, Burks DJ, Ozcan U, Kulkarni RN, Ye J, Park S, et al. Upregulation of insulin receptor substrate-2 in pancreatic beta cells prevents diabetes. J Clin Invest 2003;112(10):1521–32.
[39] Dickson LM, Rhodes CJ. Pancreatic beta-cell growth and survival in the onset of type 2 diabetes: a role for protein kinase B in the Akt? Am J Physiol Endocrinol Metab 2004;287(2):E192–8.
[40] Tuttle RL, Gill NS, Pugh W, Lee JP, Koeberlein B, Furth EE, et al. Regulation of pancreatic beta-cell growth and survival by the serine/threonine protein kinase Akt1/PKBalpha. Nat Med 2001;7(10):1133–7.
[41] González-Mariscal I, Krzysik-Walker SM, Kim W, Rouse M, Egan JM. Blockade of cannabinoid 1 receptor improves GLP-1R mediated insulin secretion in mice. Mol Cell Endocrinol 2016;423:1–10.

